

Time series classification for predictive maintenance on event logs

Antoine Guillaume^{1,2}, Christel Vrain¹,
Elloumi Wael²

Received: date / Accepted: date

Abstract Time series classification (TSC) gained a lot of attention in the past decade and number of methods for representing and classifying time series have been proposed. Nowadays, methods based on convolutional networks and ensemble techniques represent the state of the art for time series classification. Techniques transforming time series to image or text also provide reliable ways to extract meaningful features or representations of time series. We compare the state-of-the-art representation and classification methods on a specific application, that is predictive maintenance from sequences of event logs. The contributions of this paper are twofold: introducing a new data set for predictive maintenance on automated teller machines (ATMs) log data and comparing the performance of different representation methods for predicting the occurrence of a breakdown. The problem is difficult since unlike the classic case of predictive maintenance via signals from sensors, we have sequences of discrete event logs occurring at any time and the lengths of the sequences, corresponding to life cycles, vary a lot.

Keywords Sequence classification · Time series representation · Predictive maintenance · Automated Teller Machines

1 Introduction

The main goal of predictive maintenance (PdM) is to increase machine availability by minimizing unplanned maintenance due to machine failures. The benefits vary depending on the use case: for example, in a factory this leads to increased productivity, in a hospital it reduces downtime of machines that may be critical to patient health.

A classical example of PdM is the case of vibration monitoring [20]. Consider an industrial machine equipped with sensors that can measure the amplitude of vibration emitted by a piece of the machine. This signal can be used to identify

(1): Univ. Orléans, INSA Centre Val de Loire, LIFO EA 4022, F-45067, Orléans, France
E-mail: antoine.guillaume@equensworldline.com, christel.vrain@univ-orleans.fr ·
(2): equensWorldline & Worldline, Blois F-41000, France
E-mail: wael.elloumi@worldline.com

an ongoing degradation of this piece, and with knowledge of the breaking point (i.e. the amplitude where the piece will likely break), estimate the remaining time before failure. More complex systems can be monitored the same way by including more parameters, like temperature or pressure.

In this paper we consider cases where the machines we want to monitor are not equipped with sensors to capture meaningful features such as vibration, and it is not reasonable or possible to install such sensors, or to acquire the outputs of the sensors. If such machines produce logs, for example for debugging purpose, we can then use this source of data to try to identify relevant patterns in the logs, allowing to predict equipment failures. In the case of automated teller machines (ATMs in the following), we cannot directly access the sensor outputs because they are handled by a process involving transformations from the multiple communication protocols inside the ATMs and the receiving servers.

The problem we address is that of PdM, with the sole information of log data. In our application, logs are sequences of events occurring at irregular time stamps. The only available knowledge is the semantics of the events, that is either the operations performed on the ATMs or information on the state of the system. An event is generally linked to a hardware module of an ATM and a level of gravity. As stated, such a framework is applicable to a wide range of machines such as smart devices, medical equipments, servers or anything emitting logs as part of its normal operating behavior.

The dataset we use in our application of PdM with log data from ATMs has the following properties:

- It is composed of discrete time series representing the occurrences of a finite number of events through logs of event codes.
- Event codes give information about the component on which an event occurs and on the gravity of that event.
- The dataset is imbalanced with 121 recorded failures on 603 instances.
- Data was collected over an 18 month period, with some ATMs integrated during this period. Thus, the time series range from a week to 18 months.
- The frequencies of events vary between ATMs and with time.

As shown in [17], most works in predictive maintenance are either solved by using regression to estimate remaining useful life or by building a health indicator and estimating it based on recent data. Most of those approaches use data from sensors. This implies a dataset with meaningful features, and knowledge of failure time for all instances in the dataset, both of which we are lacking. To overcome these shortcomings, we chose to model PdM as a classification problem.

Many representation methods have been recently proposed for time series; some can be seen as feature extraction methods, allowing the use of classic (i.e. attribute-based) classifiers, some are dedicated to transforming time series into other time dependent representations. We review those representation methods and study their performance on our application dataset. Moreover, we study the impact of different encodings of the event codes on the results. Our contributions can be summarized as follows:

- a new dataset for predictive maintenance ¹
- a specific problem of predictive maintenance that has not yet been long studied,

¹ available on demand only for research purposes

- a review of state-of-the art representation and classification methods for time-series,
- a study of their performance on our data.

The paper is organized as follows. In Section 2, we introduce the problem of predictive maintenance and model it as a Time Series Classification Task. In Section 3, we present related work on Predictive Maintenance. Section 4 is devoted to the presentation of the data. Section 5 proposes a review of representation and classification methods for time series. Section 6 is dedicated to experiments.

In an effort to promote reproducible research, all our experiments are available online ². Dataset is available on request.

2 Predictive maintenance

The goal of PdM is to predict failure to avoid as much unplanned downtimes as possible. Regression has been extensively used to estimate the remaining duration before failure for a hardware component. But in the ATM dataset, most instances have not yet experienced failure, and we cannot compute the regression target without a timestamp indicating failure. Such data should have been discarded for applying a classic regression method.

The dataset being very unbalanced, even censored regression methods, for example based on survival analysis [16], seem hardly applicable. Thus, we preferred to model the task as a classification problem: given a time series until time T , will a failure occur in the near future?

To frame the problem as a Time Series Classification task, we need to define some time intervals. We rely on the definitions given in [24] but we adapt some of them to better fit our application.

Consider the representation given in Figure 1, we want to predict a failure that would occur in the near future, but with enough advance to have time to perform maintenance before the actual breakdown. This is the role of the predictive padding, it quantifies, at minimum, the time needed to perform a maintenance. In the context of the modeling step we define the time intervals as follows:

Let $X : \{(t_0, x_0), \dots, (t_n, x_n)\}$ a time series of length n representing the log data of a machine, with t_i a timestamp and x_i an event log.

- **Predictive padding (pp):**

The predictive padding is a quantity of time that expresses the minimum time needed to perform maintenance. To build a training/test instance for the dataset given X , we remove the data inside $[t_{n-pp}, t_n]$, and use our knowledge of the state of X at t_n to affect the label. The result is a couple (X, y) with $X = \{(t_0, x_0), \dots, (t_{n-pp}, x_{n-pp})\}$ and y a label giving the state of the machine at time t_n .

- **Infected interval (ii) = $[t_n, t_{n+ii}]$**

The infected interval is located right after the failure. All data in this interval should not be used for training or evaluation because it contains unusual data due to breakdown, maintenance or restart procedures.

² <https://gogit.univ-orleans.fr/lifo/antoine-guillaume/tsc-pdm-event-log>

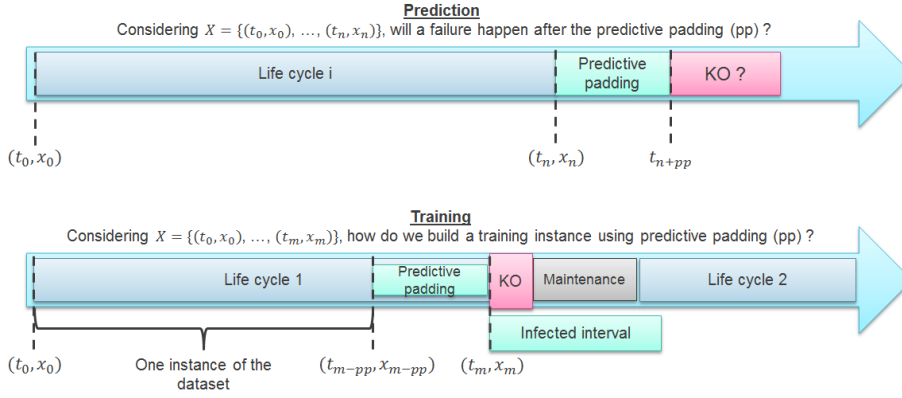


Fig. 1 Illustration of the predictive maintenance intervals for TSC.

With the above definitions, we can now frame the PdM problem as a time series classification task: considering an input time series $X = \{(t_0, x_0), \dots, (t_n, x_n)\}$ representing event logs that occurred up to time t_n , can we predict the occurrence of a failure on a component after time t_{n+pp} ?

It would be interesting not only to learn a model to discriminate classes but also to identify failure signatures present in $X = \{(t_0, x_0), \dots, (t_{n-pp}, x_{n-pp})\}$, that will influence its state after time t_n , where a failure signature is a pattern in the time or frequency domain that is characteristic of a degradation. This point is not addressed in this paper.

3 Related work

In this section we mostly focus on log based predictive maintenance approaches and techniques. The representation and classification methods used in this study will be presented in Section 5. For a more complete focus on Time Series Classification, readers are referred to the archive referenced in [3].

Supervised methods are the most common approaches for Predictive Maintenance. In [4] the authors use the prediction of an Auto-Regressive Moving Average model (ARMA) based on historical data and statistics to transform an input time series to a set of features, which is then processed by a Principal Component Analysis (PCA) before being used as inputs to a regression model to estimate remaining useful life. In [25] the authors use event logs from ATMs to extract different types of features: statistics, pattern-based features that target error message occurrences, failure similarity as a Jaccard distance to the closest failure instance, profile-based ones which takes into account the physical characteristics of the ATM and a survival probability from a Cox survival model. Those features are then given as input to classification models such as Random Forests. A similar approach is taken by [2] using a regression model to estimate the Remaining Useful Life (RUL), knowledge based and automatic feature selection approaches are also compared.

Some Predictive Maintenance systems rely on Multiple instance learning (MIL) [24] [19] [12]. Rather than learning on instances, MIL learns from bags of instances; both classification and regression can be used in this context. A positive label is

affected to a bag if at least one instance in the bag is positive. For example, [24] creates bags with a few days of logs per medical equipment.

Anomaly detection, notably applied to log data, can also be used in a PdM context. In [5], the authors present the evolving Gaussian Fuzzy Classifier (eGFC), an online semi-supervised approach for anomaly detection using logs from data centers. They use an evolving rule based approach to classify incoming logs, with rules being an ensemble of Gaussian membership function $A_j^i = G(\mu_j^i, \sigma_j^i)$, with μ_j^i the modal value and σ_j^i the dispersion of a variable j . Each rule is associated to a class C^i , with i the rule identifier. The activation of a rule is given by a triangular norm of all $A_j^i(x_j)$ rules. The rule base of eGFC can be modified based on this activation score. Existing rules can be updated or new rules can be created if no existing rule reaches an activation threshold. A distance measure is also defined between rules to merge close ones. Rules that were not activated in multiple iterations can be deleted.

4 Dataset and Preprocessing

The application we consider is predictive maintenance for ATMs. For the sake of simplicity, we do not detail all the processes that, from a given mechanical event on an ATM, lead to the generation of the event logs. Let us only write that each mechanical event leads to a sequence of event logs being generated, which will depend on the gravity of the event and the involved mechanical parts. Hence, we only present the features of the dataset necessary to the understanding of this paper.

4.1 Initial data

The data we use in this paper come from logs of hardware events emitted by multiple ATMs. An event log is composed of a timestamp and an event code (see Table 1), with an event code being a unique identifier for a type of hardware event. The dictionary of event codes is provided with the data.

timestamp	event code	Translation
2018-04-28 12:39:38	40000	Withdrawal
2018-04-28 12:41:03	2000	General State OK
2018-04-28 12:41:04	5000	Distribution Module OK
2018-04-28 12:46:34	40000	Withdrawal

Table 1 Example of logs from the ATM dataset

In our experiments, we focus on predicting failures of the distribution module, which is composed of multiple banknotes boxes and a distribution circuit with suction cups and mechanical rollers. The mechanical information recorded by sensors is sent to a computer inside the ATM, which produces logs that are sent to a platform, which translates them into event codes. Unfortunately, we cannot access

the original logs produced by the ATM. This explains why we consider only the logs of event codes. For simplicity, we only consider the distribution module in this study, but our approach for predicting failure on other components would be the same.

The dataset contains the event logs from 486 ATMs, sliced into life cycles corresponding to a period of time in which an ATM has worked correctly without failure. An ATM is composed of one or more life cycles per component, with each component having distinct life cycles. A life cycle is thus defined by a component, a start time and an end time corresponding to the failure of this component (see Figure 3 for an illustration of this process).

The dataset contains 482 life cycles yet without failure and 121 cycles with failure. Life cycles for the distribution module ranges from 7 days to 593 days, with a range of 865 to 178854 log entries. Figure 2 shows the distribution of life cycle durations for both classes and the mean time series length according to the number of days. Let us notice that the events arrive at irregular timestamps and their numbers per day vary.

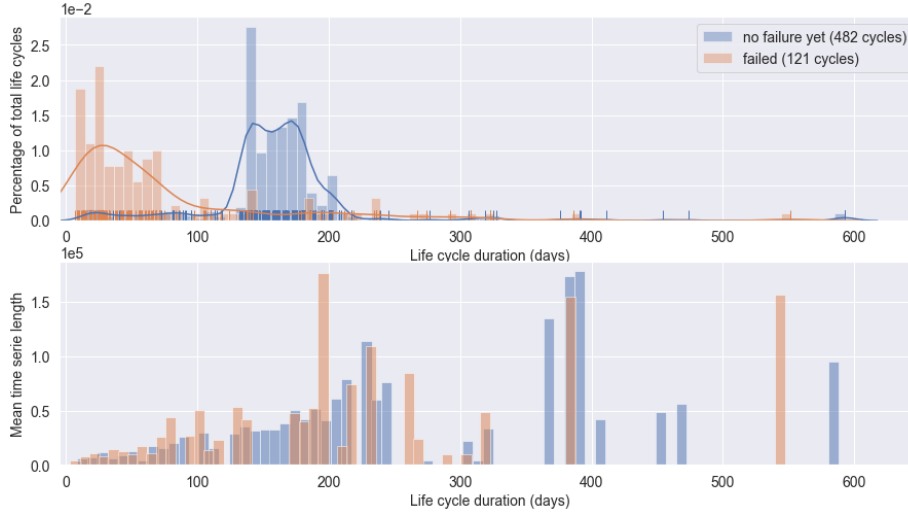


Fig. 2 The top graph shows the distribution of life cycle durations in days for life cycles with failure (orange) and yet without failure (blue). The bottom graph shows the mean time series length for bins of life cycle durations, again for both classes.

Right and left censoring are also present in the data. Right censoring corresponds to cases where, when data collection was stopped, life cycles have not yet failed. The same reasoning applies to left censoring: when the data recording started, some life cycles were already working. Hence, we do not have the data from the true beginning of those life cycles.

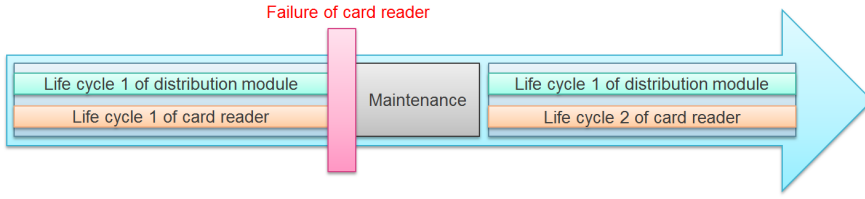


Fig. 3 An illustration of the division into life cycles. Note that the infected intervals corresponding to maintenance are removed independently of the origin of the failure, even if it was not due to a hardware component (e.g. network failure).

4.2 Slicing strategy

Depending on the known or presumed degradation process of the monitored machine, we can also apply a particular slicing strategy to better frame the predictive task.

Whole life cycle This is the basic case, where we consider the whole time series data of a life cycle. It is best suited if failure signatures (that are unknown) can occur at anytime. With the removal of the predictive padding (pp) at the end of life cycles, a life cycle X is then defined as $X = \{(t_0, x_0), \dots, (t_{n-pp}, x_{n-pp})\}$.

Subsequences If only recent data is relevant because failure signatures are supposed to happen in a given time window before a failure, we can slice time series into subsequences. Given a subsequence length L and a life cycle X as $X = \{(t_0, x_0), \dots, (t_{n-pp}, x_{n-pp})\}$, we create subsequences S starting from the end of X : $S_0 = \{(t_{n-(pp-L)}, x_{n-(pp-L)}), \dots, (t_{n-pp}, x_{n-pp})\}$ and so on. S_0 inherits the label of X , while previous subsequences, if considered, are labeled as negatives.

During early experiments, we used the whole life cycle approach along with a Piecewise Aggregate Approximation (PAA) [11] to even the length of the time series. Due to the distribution of the data, a bias was introduced when using a PAA. Most life cycles with failure have a low number of data points compared to non-failure ones because of their small duration. The averaging performed by the PAA produced less unique values due to shorter aggregation windows and a smaller variety of event codes.

A simple decision tree based on the original length of the time series scored 65% balanced accuracy in a 10 fold cross validation, while a decision tree based on the number of unique values after PAA scored 83% balanced accuracy, clearly showing the introduced bias. For the experiments in this paper, we use the subsequence strategy detailed hereafter in which such a bias was not identified.

4.3 Preprocessing

To implement the subsequences approach, we use for each life cycle the last 21 days of data with a resample frequency of 20 minutes, which naturally make all the time series even in length. We investigate the effect of the subsequence duration and resampling frequency in section 6. If multiple event codes are present in a

resampling window, we take the average value, if no codes are present, we define a filling value, depending on the data encodings. Life cycles with less than 21 days of data are dismissed, which reduce our dataset to 465 negative and 89 positive instances.

Before those operations, we apply a temporal alignment of the life cycles. After applying the predictive padding, we remove all data of the current day for each cycle, so they are aligned daily. This modify our problem formulation, making the predictive padding a time window $[pp; pp + 24h[$.

4.3.1 Data encoding

Four encodings are considered, each with a filling value for resampling windows with no events. We will investigate in Section 6 their interest in regard to our classification problem. Figure 4 illustrates the different encodings.

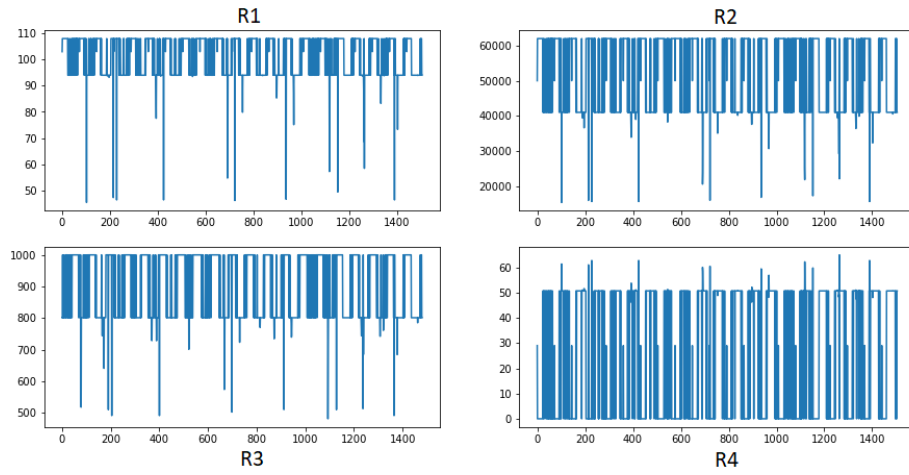


Fig. 4 Visual comparison between the different data encodings after selecting the last 21 days of data and resampling

- **R1** converts the event codes into range $[0, n]$ with n the number of event codes. It is made by sorting the list of codes and affecting to each code its position in the sorted list. The fill value will be $n + 1$ in this case.
- **R2** is the "raw" representation, it simply takes the numeric value of the code as it is. A code with value 4000 keeps this value. In this case, the fill value is the maximum code plus 1000, as hardware components codes are separated by a value of 1000.
- **R3** sorts the event codes by gravity while R2 and R1 implicitly sort event codes by components because of how the dictionary is made. By default, we take all codes from a same gravity and affect them a value by sorting them as we did for all the codes in R1. We do it again for the next gravity level, adding an arbitrary value (here 200) for each level to separate the gravity levels. We chose to process gravity levels in the following order: KO, Warning, OK and Withdrawals. The fill value is one level above the Withdrawals codes.

- **R4** affects a unique random value between 0 and $n + 1$ to each code. We use $n + 1$ to affect a random fill value.

5 Methods

In this section we briefly present the representation and classification techniques that we use for the experiments. Readers are referred to original papers for the details of each method.

The focus of this paper being time series classification, we do not cover other techniques such as survival analysis, semi-supervised regression techniques or Health-Index estimation that could be used to tackle issues related to censored data.

5.1 Change of Representation techniques

In our experiments, the techniques discussed below will be used after performing the preprocessing steps described in Section 4.3. In the following, we consider $X = \{x_1, \dots, x_n\}$ a time series of size n .

5.1.1 Time series approximation

Symbolic Aggregate approXimation (SAX) [13] is classically used to transform a time series of length n into a string of arbitrary length o . It first uses PAA [11] to produce X' a series of length o and then given the size a of the alphabet it computes discretization bins on the values of X' . The result is a time series of length o with a different values, the bins allowing to assign to each value of X' a particular letter of the alphabet. Multiple strategies exist to define the range of the bins, all are based on the distribution of the values in X' :

- Uniform range: all bins have identical ranges, this range is obtained by dividing the value distribution in a equal parts.
- Percentile range: all bins have the same number of points inside their ranges, bins edges are defined using the percentiles of X .
- Normal range: here, bins edges are percentiles from a standard normal distribution.

Note that the alphabet can also be numeric so the approximation can be used for numeric applications. Another discretization technique, called **Symbolic Fourier Approximation (SFA)** [22] also exists, it relies on discrete Fourier transformation to extract Fourier coefficients from an input time series and transforms it into a word of discrete Fourier coefficients. In our experiments, we do not use PAA before applying SAX or SFA.

5.1.2 Time series to images

Inspired by the recent success of image classification, methods transforming time series into images have been developed, allowing to apply image classifiers for time series classification. In the experiments, we call an image transformation "flat" when we flatten the output image to obtain one feature per pixel, and use them as independent features.

Gramian Angular Fields (GAF) [26] aims at creating a matrix containing temporal correlations between each couple (x_i, x_j) of a time series X of size n . The size of the matrix $n \times n$ will be the size of the image and each value will be encoded into colors, creating the image. First, the data is re-scaled in range $[-1, 1]$ so that it can be used as an input of the arc-cosine function. Then, each point x_i is converted into polar coordinates by:

$$\phi = \arccos(x_i), \quad r = \frac{i}{n} \quad (1)$$

with ϕ the angular cosine and r the radius. To build the matrix M , GAF takes the trigonometric sum (or difference) of each couple:

$$M_{i,j} = \cos(\phi_i + \phi_j) = \cos(\phi_i)\cos(\phi_j) - \sin(\phi_i)\sin(\phi_j) \quad (2)$$

Recurrence Plots [7] proposes to build a matrix containing the pairwise distances between parts of a time series X of length n . Those parts are called trajectories and they are defined as:

$$\vec{x}_i = \{x_i, x_{i+\tau}, \dots, x_{i+(m-1)\tau}\} \quad \forall i \in \{1, \dots, n - (m-1)\tau\} \quad (3)$$

with m the "dimension" parameter and τ the "time delay" parameter. Once those trajectories are computed, the Recurrence Matrix M is defined as:

$$M_{i,j} = \Theta(\varepsilon - \|\vec{x}_i - \vec{x}_j\|) \quad (4)$$

with Θ the Heaviside function (defined by $\Theta(x < 0) = 0$ and $\Theta(x \geq 0) = 1$) and ε a parameter representing a threshold for a minimum distance between points.

5.1.3 Sliding operations

Some techniques use sliding window operations on an input time series, to generate a new time series in which some patterns may appear.

Matrix Profile (MP) [27] takes as input a time series $X = \{x_1, \dots, x_n\}$ and a window size w and generates a new time series $X' = \{x'_1, \dots, x'_{n-w}\}$ in which x'_i represents the minimum distance between the subsequence $\{x_i, \dots, x_{i+w}\}$ and any other subsequences of size w inside X . The brute force approach being intractable, multiple algorithms providing speed-ups through lower bounding and other techniques have been developed, which make the time complexity of the MP be linear with input length.

Random Convolutional Kernel Transform (ROCKET) [6] randomly initializes a huge number (10.000 by default) of convolutional kernels K , $K = \{l, \{w_1, \dots, w_l\}, b, d, p\}$, with l the length of the kernel, w its weights, b the bias, d the dilation and p a boolean determining whether padding is used or not. If N kernels are generated, ROCKET will output a 1-dimensional array containing $2N$ features, since 2 features are extracted for each convolution of the input by a kernel. For a time series $X = \{x_1, \dots, x_n\}$ and a kernel $K = \{l, \{w_1, \dots, w_l\}, b, d, p\}$, the output of the convolution computed from position i is defined:

$$c_i = b + \sum_{j=1}^l w_j \times X_{i+(j \times d)} \quad (5)$$

When padding is used, X is completed with zeros at the beginning and the end of X so that the middle of the kernel is centered on every point, as stated in [6]. The two features extracted from a kernel K are the maximum value of the (c_i) and the proportion of positive values. This operation is repeated for each of the N kernels that were randomly initialized.

5.2 Classification techniques

We suppose that the reader has knowledge on the most widely used classification algorithms (i.e. k-nearest neighbors (KNN), support vector machines (SVM), random forest (RF), etc.) and we focus on algorithms that can be used for time series classification.

Time series Forest (TSF) [1] applies the principle of random forests to time series data. To make a split, RF classically considers \sqrt{M} features at each node with M the total number of features of the input. In TSF, M is defined as the length of the input time series. A tree will randomly sample \sqrt{M} starting positions and \sqrt{M} interval lengths for input time series, giving M intervals on which statistics like mean, standard deviation and slope are computed, thus giving candidates to be considered for the split.

Random Interval Spectral forEst (RISE) [14] uses the same approach of building trees based on features extracted from intervals, but extracts time and frequency domain features with methods such as auto-correlation or power spectrum.

Bag-of-SFA Symbols in Vector Space (BOSSVS) [21] uses a text mining approach to solve a time series classification problem. From an input time series X , a word size l , an alphabet a and a window size w , it produces a histogram of symbolic Fourier approximation (SFA) words. More precisely, X is divided into moving windows of size w , each window is then transformed to a word of size l using SFA with alphabet a . The histogram is then built upon all the words extracted.

To discriminate classes, the histograms of each class are added up and a tf-idf (term frequency inverse document frequency) vector is computed. A new sample is predicted as the class leading to the highest cosine similarity between its tf-idf vector and the tf-idf vectors of the sample.

For a time series X , a histogram B_X and a SFA word x , the term frequency (tf) of x inside a class C is defined as:

$$tf(x, C) = \begin{cases} 1 + \log(\sum_{X \in C} B_X(x)) & \text{if } \sum_{X \in C} B_X(x) > 0 \\ 0 & \text{otherwise} \end{cases}$$

with $B_X(x)$ the value of x in the histogram of B_X . The inverse document frequency (idf) is defined by:

$$idf(x, C) = \log\left(1 + \frac{|Classes|}{|\{C|X \in C \wedge B_X(x) > 0\}|}\right) \quad (6)$$

The idf of a SFA word x for a class C represents the proportion of classes in which this word occurs; high values of idf mean that a word is specific to a few classes relatively to the total number of classes. With $tfidf(x, C) = tf(x, C).idf(x, C)$, the BOSS-VS distance can then be defined as a cosine similarity:

$$D_{BOSSVS}(X, C) = \frac{\sum_{x \in X} tf(x, X) \cdot (tfidf(x, C) + 1)}{\sqrt{\sum_{x \in X} (tf(x, X))^2} \cdot \sqrt{\sum_{x \in C} (tfidf(x, C))^2}} \quad (7)$$

Time Series Combination of Heterogeneous and Integrated Embedding Forest (TS-CHIEF) [23] is another ensemble, tree based algorithm. The authors define multiple splitting methods at node level, based on popular algorithms used in TSC. To split a node, those different methods are randomly initialized multiple times, and the one that maximizes a splitting criterion is chosen as the splitting method for this node. The algorithms that are re-defined as splitting methods in TS-CHIEF are: Proximity Forest, BOSS-VS and RISE. The methodology is close to the one used in HIVE-COTE [15], but with fewer splitting methods and random initializations, which presents a huge gain in time complexity without significative loss in performance.

6 Experiments

The experiments we perform aims at answering the following questions.

- What are the best combinations of representation techniques and classifiers for the problem at hand? (Subsection 6.3.1)
- More precisely, given a family of representation techniques, which ones give the best results for the application? (Subsection 6.3.2)
- What are the performance of the time-series classifiers: TSF, RISE, BOSSVS, TS-CHIEF? (Subsection 6.3.1)
- Among the 4 encodings proposed in Section 4.3.1, which one is the most suited to our problem? (Subsection 6.3.3)
- What is the influence of the predictive padding and the subsequence window length ? (Subsection 6.3.4)

6.1 Protocol

Starting with the raw data described in Section 4, we apply a predictive padding of 48 hours. Then, for each life cycle we remove the data of the current day, thus allowing us to have a daily temporal alignment. Next, we select the last 21 days of data for each life cycle and perform a resampling with a frequency of 20 minutes. Life cycles with less than 21 days of data are dismissed.

For each combination of representation and classification algorithms we wish to test, we use a 10-fold cross validation to extract the balanced accuracy, the f1-score and the critical failure index (CFI), defined by $(fp + fn)/(tp + fp + fn)$, which is not affected by the number of true negatives. We then repeat this protocol for each data encoding described in Section 4.3.1. The code for the experiments is available online ³.

6.2 Methods

We aim at studying the interest of representation techniques for our application of failure detection in ATMs. These methods can be distinguished according to the type of outputs they produce (time series, features or images) and we combine them with different classifiers, depending on the type of outputs:

- Feature-based representations (ROCKET, flattened images) generate a new set of features and are combined with classic classifiers: SVM, RF, Ridge and kNN with Euclidean distance.
- Image representations (GAF, recurrence plots) are combined with ResNet50V2 [9], a deep residual network architecture.
- Time series representations (SFA, SAX and Matrix Profile) generate a new time series and are combined with TSF, RISE, BOSSVS, TS-CHIEF and kNN with Euclidean distance. We also use InceptionTime [10], an ensemble of deep Convolutional Neural Network (CNN) models using Inception modules.
- Representation stacking is also tested, for example using Matrix Profile before ROCKET. The features generated by most of the representation methods are difficult to interpret and thus we wonder whether stacking them with other methods could lead to interesting results. Let us notice that stacking makes the interpretation of the outputs much more difficult.

In the following, we call method a combination of representation and classification algorithms. For instance SAX ROCKET KNN represents the application of SAX on the input time series, followed by the application of ROCKET, thus generating features that can be given as inputs to kNN.

6.3 Experimental results

6.3.1 Best Methods

In this section, we present the best methods for the ATM dataset based on our experimental results. The results and parameters of all methods are available in Appendix A. Figure 5 shows the ranking of the top performing methods based on the mean critical failure index over all non-random data encodings (R1, R2, R3). If we consider only R1, which is the best encoding (see Section 6.3.3), then Rocket SVM achieves the best result in terms of CFI.

The F1 score obtained by the best algorithms are given in Table 2. For sake of simplicity, we do not include R4 (random encoding) that gives the worst results.

³ <https://gogit.univ-orleans.fr/lifo/antoine-guillaume/tsc-pdm-event-log>

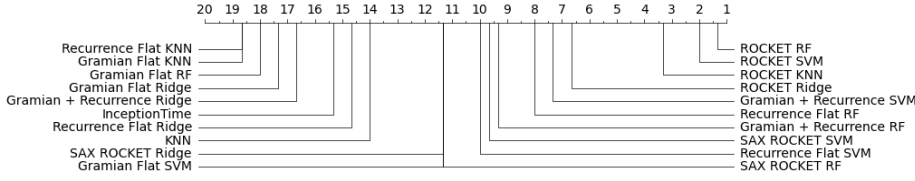


Fig. 5 Average ranking of methods based on the mean critical failure index on the non-random data encodings (top 20 for readability)

Name	F1 score with R1	F1 score with R2	F1 score with R3
ROCKET SVM	0.838(+/- 0.085)	0.800(+/- 0.068)	0.683(+/- 0.164)
KNN	0.757(+/- 0.095)	0.594(+/- 0.158)	0.615(+/- 0.075)
TS-CHIEF	0.757(+/- 0.118)	0.674(+/- 0.091)	0.430(+/- 0.218)
Recurrence Flat RF	0.733(+/- 0.107)	0.734(+/- 0.085)	0.671(+/- 0.061)

Table 2 Performance of the best methods on the ATM dataset. R4 and many ROCKET variants are not included.

ROCKET based methods are the top performers for our application. To understand this fact, we made a closer inspection of the kernels that were generated. Figure 6 shows how the two features of one of the most discriminant kernel⁴ discriminate the data. We see that the maximum value obtained by the kernel is an important feature: the ATMs regularly perform restart operations and in most cases, the maximum value of this kernel occurs around the last check-up or restart process. Other families of behavior seem to emerge from kernels with different parameters, suggesting that ROCKET identifies some patterns, either local (with the max feature) or global (with the ppv feature), potentially leading to failures. Other methods also give acceptable results such as flattened images, TS-CHIEF and kNN with Euclidean distance.

Aside from predictive performance, another point to consider is the time complexity of the different methods. Experiments were run on a DELL PowerEdge R730 on Debian 9.x with 2 XEON E5-2630 Corei7 and 32GB of RAM. We recorded fit and prediction times on each cross validation split and we give in Table 3 the mean of the total time (fit+predict) in seconds computed on all splits, for all data encodings (R1, R2, R3 and R4). ResNet50V2 and InceptionTime were run using a Tesla P100.

name	Mean fit + predict time (seconds)
KNN	0.182(+/- 0.006)
Recurrence Flat RF	4.670(+/- 0.068)
TSF	35.29(+/- 0.434)
ROCKET SVM	213.9(+/- 0.653)

Table 3 Run time of the top performing methods

⁴ The importance of a kernel is assessed by the sum of the information gain of its two features, max and ppv.

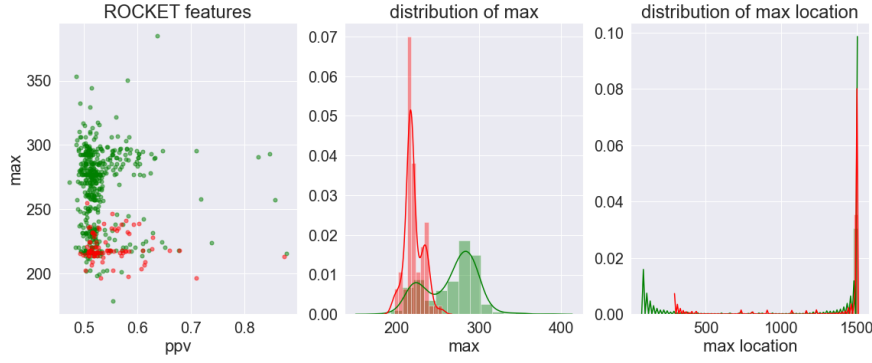


Fig. 6 From left to right - green the negative class and red the positive class: the two features (ppv on axis x and max on axis y) generated by one of the most discriminant kernel of ROCKET, the distribution of the maximum value for each class, the distribution of the location of the maximum value inside the convolved input.

Looking at the top methods, kNN offers the best run-time for the 3rd best CFI score outside ROCKET methods. ROCKET SVM, which has the best performance for the encoding R1, and achieves a reasonable run-time of less than 4 minutes.

6.3.2 Influence of representation techniques

We study the influence on performance of the different representation methods, presented in Subsection 5.1.

For time series representations, in most cases, Matrix profile (MP), SAX and SFA have a negative impact on the performance of time series classifiers as seen in Table 4. While it seems reasonable that approximation techniques such as SAX and SFA do not improve performance, the negative impact of MP could either mean that it is not interesting for our learning task, or that we did not find a suitable window length.

name	F1 score R1	F1 score R2	F1 score R3
MP TSF	0.491(+/- 0.120)	0.263(+/- 0.129)	0.347(+/- 0.236)
TSF	0.701(+/- 0.145)	0.599(+/- 0.172)	0.503(+/- 0.170)
MP KNN	0.432(+/- 0.087)	0.239(+/- 0.191)	0.325(+/- 0.180)
KNN	0.757(+/- 0.095)	0.594(+/- 0.158)	0.615(+/- 0.075)

Table 4 Effect of Matrix profile on time series classifiers

Considering image representations, Recurrence plot is above Gramian Angular Fields as shown in Table 5, when used as flattened images. This tendency is reversed when using ResNet50V2.

For feature based representations, ROCKET is the best one, as shown in Table 2. Representation stacking does not have a positive impact compared to individual representation methods. For example applying MP before using any feature

name	F1 score R1	F1 score R2	F1 score R3
Recurrence Flat RF	0.733(+/- 0.107)	0.734(+/- 0.085)	0.671(+/- 0.061)
Gramian Flat SVM	0.691(+/- 0.075)	0.720(+/- 0.089)	0.687(+/- 0.062)
Gramian ResNetV2	0.513(+/- 0.158)	0.404(+/- 0.308)	0.452(+/- 0.341)
Reccurence ResNetV2	0.239(+/- 0.265)	0.317(+/- 0.293)	0.216(+/- 0.229)

Table 5 Performance of the image representations

based representation leads to worse results than without MP. Combining image representations also do not achieve better results.

6.3.3 Influence of data encodings

In Subsection 4.3.1, we have proposed 4 encodings for the events emitted by the ATMs and we aim at studying their influence.

Table 6 shows the performance of each encoding through 4 criteria: the minimum and mean CFI obtained on all methods, the number of times the encoding has been ranked first and its mean rank. We can observe that R1 is the best one, followed by R2, which is quite close and that R4 is the worst one. From those results, we can deduce the following points:

- Encoding event codes by their gravity level (R3) is not more efficient than by their components (R1, R2).
- The notion on scale between event codes values, that is the choice between R1 and R2 encodings, has an impact for most methods. Looking at the full results, we cannot identify families of methods that perform best with one kind of encodings (for instance kNN performs best with R1 while SAX-kNN performs best on R2 and SAX-Rocket-RF performs best with R1).
- The lower results of the random representation (R4) implies that a relation does exist between some patterns of event codes and failures.

Note that we apply min-max normalization before classification algorithms where different feature scales can introduce bias, such as kNN. The last tables in appendix A give the configuration of each method, including whether or not they use min-max normalization before classification.

	R1	R2	R3	R4
Mean CFI	0.519(+/- 0.121)	0.566(+/- 0.171)	0.656(+/- 0.141)	0.707(+/- 0.155)
Min CFI	0.268	0.318	0.385	0.464
Rank 1 (# times)	31	14	0	0
Mean rank	1.31	1.91	3.11	3.73

Table 6 Performance of the data encodings on critical failure index (CFI) and ranks within the same methods

6.3.4 Influence of the predictive padding and preprocessing

We study the influence of the predictive padding size, the window size and resample frequency. We rely on the two most efficient methods that are ROCKET SVM and KNN. Figure 7 shows the influence of these factors on F1 Score.

Looking at the number of days used in preprocessing to build input time series, ROCKET SVM performance improves as the size increases up to 21 days, then it starts to decrease. This could be due to the fact that when the number of days increases, the size of our dataset is reduced, as life cycles of less than the given number of days are discarded.

Both methods seem to benefit of small values of predictive padding (compared to no predictive padding), it could be that removing some data at the end of the life cycles prevent the algorithm from overfitting on irrelevant patterns based on the breakdown process.

Concerning the resample frequency, KNN benefits from the smaller and thus, more approximated, time series made with higher resampling value. This parameter could be important when using algorithms based on similarity between time series to allow for better generalization.

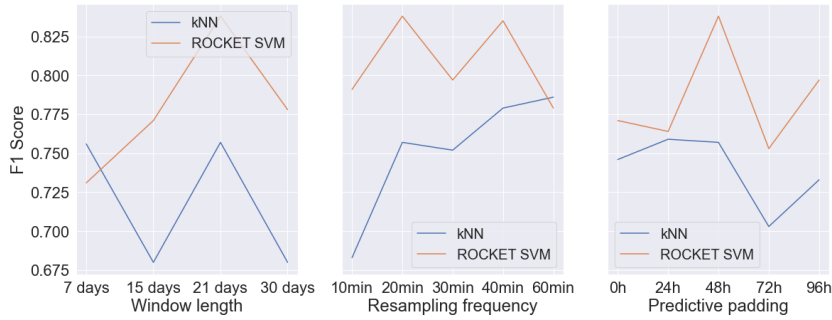


Fig. 7 From left to right, effect of the window length, resampling frequency and predictive padding on F1 Score with ROCKET SVM and KNN

7 Conclusion & Future work

The goal of this study was to formulate a predictive maintenance problem based on time series of event logs and conduct multiple experiments to find the most suited approaches for the application (predict failure for ATMs). Our experimental results show that using ROCKET, with a SVM and a data encoding sorted by hardware components, seems to be the most efficient approach. Nevertheless, the features generated by ROCKET are not easily interpretable and this is a drawback since interpretability is an important property for predictive maintenance. Number of methods have been recently developed for time series interpretability [18,8], either global methods, which look at relations learned by an estimator, or local methods, which study how an estimator behaves if inputs are slightly modified. Global methods do not seem adapted as features produced by ROCKET and fed to

an estimator will not be directly interpretable. Concerning local methods, studying the effects of small variations of the inputs on the relevant features generated by ROCKET is not trivial. We aim at developing a method that combines the efficiency of methods like ROCKET and interpretability capacities in order to extract patterns highlighted by kernels sharing similar parameters.

Our current formulation of predictive maintenance as a time series classification problem impose, by means of the predictive padding, a lower bound on the time before failure. Thus, it allows to predict a failure early enough to perform maintenance. We would now like to study the introduction of an upper bound, so that we do not predict failure too early, avoiding "unnecessary" maintenance.

Acknowledgements We thank Naly Raliravaka (LIFO) for his help on setting up the experimental environments and online repository. We thank members of the ATM team at equensWorldline, Arnaud Celier, Olivier Hubert, Armino Martins, Philippe Carrez and Laurent Desnouailles for discussions about the ATMs, Frank Charles and Ghislaine Le Goff for their contribution on the ATM data acquisition, Didier Noellec and Eric Prieur for their support in the project management. This work was supported by the ANRT CIFRE grant n°2019/0281 in partnership with equensWorldline and the University of Orléans.

References

1. A time series forest for classification and feature extraction. *Information Sciences* **239**, 142 – 153 (2013)
2. Log-based predictive maintenance in discrete parts manufacturing. *Procedia CIRP* **79**, 528 – 533 (2019)
3. Anthony Bagnall Jason Lines, W.V., Keogh, E.: The UEA & UCR Time Series Classification Repository. URL www.timeseriesclassification.com
4. Baptista, M., Sankararaman, S., de Medeiros, I., Nascimento Jr, C., Prendinger, H., Henriques, E.: Forecasting fault events for predictive maintenance using data-driven techniques and arma modeling. *Computers & Industrial Engineering* **115** (2017)
5. Decker, L., Leite, D., Giommi, L., Bonacorsi, D.: Real-time anomaly detection in data centers for log-based predictive maintenance using an evolving fuzzy-rule-based approach. In: 2020 IEEE International Conference on Fuzzy Systems (FUZZ-IEEE), pp. 1–8 (2020)
6. Dempster, A., Petitjean, F., Webb, G.: Rocket: Exceptionally fast and accurate time series classification using random convolutional kernels (2019)
7. Eckmann, J.P., Kamphorst, S.: Recurrence plots of dynamical systems. *Europhysics Letters (epl)* **4**, 973–977 (1987)
8. Guillemé, M., Masson, V., Rozé, L., Termier, A.: Agnostic local explanation for time series classification. In: 2019 IEEE 31st International Conference on Tools with Artificial Intelligence (ICTAI), pp. 432–439 (2019)
9. He, K., Zhang, X., Ren, S., Sun, J.: Identity mappings in deep residual networks. In: B. Leibe, J. Matas, N. Sebe, M. Welling (eds.) *Computer Vision – ECCV 2016*, pp. 630–645. Springer International Publishing, Cham (2016)
10. Ismail Fawaz, H., Lucas, B., Forestier, G., Pelletier, C., Schmidt, D., Weber, J., Webb, G., Idoumghar, L., Muller, P.A., Petitjean, F.: Inceptiontime: Finding alexnet for time series classification. *Data Mining and Knowledge Discovery* pp. 1–27 (2020)
11. Keogh, E., Chakrabarti, K., Pazzani, M., Mehrotra, S.: Dimensionality reduction for fast similarity search in large time series databases. *Knowledge and Information Systems* **3** (2002)
12. Korvesis, P., Besseau, S., Vazirgiannis, M.: Predictive maintenance in aviation: Failure prediction from post-flight reports. In: 2018 IEEE 34th International Conference on Data Engineering (ICDE), pp. 1414–1422 (2018)
13. Lin, J., Keogh, E., Wei, L., Lonardi, S.:
14. Lines, J., Taylor, S., Bagnall, A.: Hive-cote: The hierarchical vote collective of transformation-based ensembles for time series classification. In: 2016 IEEE 16th International Conference on Data Mining (ICDM), pp. 1041–1046 (2016)

15. Lines, J., Taylor, S., Bagnall, A.: Time series classification with hive-cote: The hierarchical vote collective of transformation-based ensembles **12**(5) (2018)
16. Ma, Z., Krings, A.W.: Survival analysis approach to reliability, survivability and prognostics and health management (phm). In: 2008 IEEE Aerospace Conference, pp. 1–20 (2008)
17. Miller, K., Dubrawski, A.: System-level predictive maintenance: Review of research literature and gap analysis (2020)
18. Mujkanovic, F., Doskoč, V., Schirneck, M., Schäfer, P., Friedrich, T.: timexplain – a framework for explaining the predictions of time series classifiers (2020)
19. Murray, J.F., Hughes, G.F., Kreutz-Delgado, K.: Machine learning methods for predicting failures in hard drives: A multiple-instance application. *J. Mach. Learn. Res.* **6**, 783–816 (2005)
20. Orhan, S., Aktürk, N., Çelik, V.: Vibration monitoring for defect diagnosis of rolling element bearings as a predictive maintenance tool: Comprehensive case studies. *NDT & E International* **39**(4), 293 – 298 (2006)
21. Schäfer, P.: Scalable time series classification. *Data Mining and Knowledge Discovery* **30**(5), 1273–1298 (2016)
22. Schäfer, P., Höggqvist, M.: Sfa: A symbolic fourier approximation and index for similarity search in high dimensional datasets. Association for Computing Machinery, New York, NY, USA (2012)
23. Shifaz, A., Pelletier, C., Petitjean, F., Webb, G.: Ts-chief: a scalable and accurate forest algorithm for time series classification. *Data Mining and Knowledge Discovery* (2020)
24. Sipos, R., Fradkin, D., Moerchen, F., Wang, Z.: Log-based predictive maintenance. In: Proceedings of the 20th ACM SIGKDD International Conference on Knowledge Discovery and Data Mining, KDD '14, p. 1867–1876. Association for Computing Machinery, New York, NY, USA (2014)
25. Wang, J., Li, C., Han, S., Sarkar, S., Zhou, X.: Predictive maintenance based on event-log analysis: A case study **61**(1) (2017)
26. Wang, Z., Oates, T.: Encoding time series as images for visual inspection and classification using tiled convolutional neural networks (2015)
27. Yeh, C.M., Zhu, Y., Ulanova, L., Begum, N., Ding, Y., Dau, H.A., Silva, D.F., Mueen, A., Keogh, E.: Matrix profile i: All pairs similarity joins for time series: A unifying view that includes motifs, discords and shapelets. In: 2016 IEEE 16th International Conference on Data Mining (ICDM), pp. 1317–1322 (2016)

Appendices

A Experiment Results

name	Mean fit + predict time (seconds)
KNN	0.182(+/- 0.006)
SAX KNN	1.668(+/- 0.024)
SFA KNN	1.861(+/- 0.025)
SFA TSF	2.537(+/- 0.042)
Recurrence Flat KNN	3.622(+/- 0.117)
Recurrence Flat Ridge	3.684(+/- 0.142)
MP KNN	3.696(+/- 0.030)
Gramian Flat KNN	3.789(+/- 0.121)
Gramian Flat Ridge	3.911(+/- 0.157)
BOSSVS	4.470(+/- 0.070)
Recurrence Flat SVM	4.526(+/- 0.175)
Recurrence Flat RF	4.670(+/- 0.068)
SAX BOSSVS	5.971(+/- 0.060)
Gramian + Recurrence KNN	6.096(+/- 0.248)
Gramian + Recurrence Ridge	6.112(+/- 0.264)
Gramian + Recurrence SVM	6.128(+/- 0.265)
Gramian Flat SVM	6.347(+/- 0.193)
MP BOSSVS	6.708(+/- 0.085)
Gramian + Recurrence RF	6.822(+/- 0.267)
Gramian Flat RF	7.396(+/- 0.090)
MP Gramian + Recurrence SVM	12.18(+/- 0.365)
MP Gramian + Recurrence KNN	12.52(+/- 0.357)
MP Gramian + Recurrence Ridge	12.98(+/- 0.363)
MP Gramian + Recurrence RF	13.47(+/- 0.303)
MP TSF	34.29(+/- 0.193)
TSF	35.29(+/- 0.434)
SAX TSF	36.93(+/- 0.494)
MP ROCKET Ridge	181.6(+/- 1.220)
MP ROCKET SVM	181.6(+/- 0.557)
MP ROCKET KNN	182.0(+/- 0.594)
MP ROCKET RF	184.4(+/- 0.608)
ROCKET Ridge	208.1(+/- 0.731)
SAX ROCKET RF	208.3(+/- 0.353)
ROCKET KNN	208.5(+/- 0.945)
SAX ROCKET SVM	208.7(+/- 0.408)
SAX ROCKET Ridge	208.9(+/- 1.694)
SAX ROCKET KNN	209.6(+/- 0.577)
ROCKET SVM	213.9(+/- 0.653)
ROCKET RF	214.3(+/- 1.001)
Recurrence ResNetV2	273.5(+/- 32.11)
Gramian ResNetV2	281.3(+/- 31.21)
InceptionTime	397.3(+/- 37.54)
RISE	633.2(+/- 11.83)
SAX RISE	644.9(+/- 21.05)
MP RISE	650.2(+/- 19.64)
TS CHIEF	14408(+/- 143.4)

Table 7 Mean run time for all methods

name	balanced accuracy R1	balanced accuracy R2	balanced accuracy R3	balanced accuracy R4
ROCKET RF	0.913(+/- 0.054)	0.921(+/- 0.030)	0.880(+/- 0.060)	0.768(+/- 0.072)
ROCKET SVM	0.905(+/- 0.062)	0.883(+/- 0.046)	0.801(+/- 0.103)	0.779(+/- 0.095)
Recurrence Flat Ridge	0.905(+/- 0.030)	0.889(+/- 0.040)	0.860(+/- 0.057)	0.833(+/- 0.046)
Gramian + Recurrence RF	0.899(+/- 0.062)	0.896(+/- 0.044)	0.880(+/- 0.061)	0.814(+/- 0.072)
Gramian Flat Ridge	0.892(+/- 0.039)	0.895(+/- 0.041)	0.839(+/- 0.063)	0.817(+/- 0.078)
Gramian + Recurrence Ridge	0.892(+/- 0.035)	0.894(+/- 0.041)	0.875(+/- 0.048)	0.838(+/- 0.025)
ROCKET Ridge	0.891(+/- 0.043)	0.919(+/- 0.049)	0.842(+/- 0.060)	0.778(+/- 0.091)
Gramian + Recurrence SVM	0.883(+/- 0.062)	0.894(+/- 0.064)	0.846(+/- 0.036)	0.804(+/- 0.069)
SAX ROCKET Ridge	0.864(+/- 0.056)	0.910(+/- 0.049)	0.829(+/- 0.055)	0.784(+/- 0.097)
ROCKET KNN	0.848(+/- 0.067)	0.889(+/- 0.059)	0.802(+/- 0.100)	0.689(+/- 0.080)
Gramian Flat SVM	0.847(+/- 0.059)	0.863(+/- 0.065)	0.842(+/- 0.038)	0.794(+/- 0.072)
SAX ROCKET RF	0.843(+/- 0.066)	0.802(+/- 0.074)	0.721(+/- 0.081)	0.730(+/- 0.073)
SAX ROCKET SVM	0.843(+/- 0.063)	0.870(+/- 0.086)	0.761(+/- 0.059)	0.753(+/- 0.089)
Recurrence Flat SVM	0.840(+/- 0.047)	0.865(+/- 0.083)	0.808(+/- 0.075)	0.750(+/- 0.074)
Recurrence Flat RF	0.839(+/- 0.068)	0.841(+/- 0.070)	0.843(+/- 0.056)	0.792(+/- 0.077)
KNN	0.835(+/- 0.059)	0.725(+/- 0.080)	0.784(+/- 0.048)	0.603(+/- 0.060)
TS-CHIEF	0.833(+/- 0.080)	0.774(+/- 0.058)	0.650(+/- 0.090)	0.564(+/- 0.054)
MP ROCKET Ridge	0.819(+/- 0.085)	0.735(+/- 0.138)	0.734(+/- 0.136)	0.630(+/- 0.100)
Recurrence Flat KNN	0.816(+/- 0.073)	0.809(+/- 0.074)	0.686(+/- 0.066)	0.646(+/- 0.057)
Gramian Flat KNN	0.810(+/- 0.068)	0.817(+/- 0.075)	0.689(+/- 0.079)	0.780(+/- 0.075)
SAX ROCKET KNN	0.806(+/- 0.085)	0.821(+/- 0.065)	0.670(+/- 0.039)	0.717(+/- 0.063)
Gramian + Recurrence KNN	0.804(+/- 0.076)	0.792(+/- 0.083)	0.687(+/- 0.070)	0.746(+/- 0.086)
Gramian Flat RF	0.803(+/- 0.068)	0.790(+/- 0.071)	0.770(+/- 0.049)	0.770(+/- 0.070)
BOSSVS	0.801(+/- 0.029)	0.792(+/- 0.053)	0.698(+/- 0.099)	0.679(+/- 0.065)
MP ROCKET SVM	0.799(+/- 0.082)	0.724(+/- 0.116)	0.700(+/- 0.074)	0.626(+/- 0.140)
InceptionTime	0.792(+/- 0.077)	0.836(+/- 0.103)	0.698(+/- 0.118)	0.574(+/- 0.100)
TSF	0.790(+/- 0.096)	0.733(+/- 0.092)	0.686(+/- 0.087)	0.632(+/- 0.079)
SFA TSF	0.788(+/- 0.064)	0.710(+/- 0.088)	0.610(+/- 0.061)	0.637(+/- 0.100)
MP ROCKET RF	0.780(+/- 0.092)	0.760(+/- 0.127)	0.704(+/- 0.124)	0.608(+/- 0.119)
SFA KNN	0.780(+/- 0.080)	0.783(+/- 0.044)	0.612(+/- 0.066)	0.654(+/- 0.061)
SAX TSF	0.776(+/- 0.065)	0.751(+/- 0.034)	0.629(+/- 0.065)	0.619(+/- 0.069)
SAX BOSSVS	0.774(+/- 0.046)	0.734(+/- 0.083)	0.606(+/- 0.084)	0.694(+/- 0.082)
MP Gramian + Recurrence Ridge	0.753(+/- 0.113)	0.738(+/- 0.065)	0.701(+/- 0.062)	0.646(+/- 0.089)
SAX KNN	0.739(+/- 0.075)	0.631(+/- 0.061)	0.688(+/- 0.079)	0.600(+/- 0.048)
MP ROCKET KNN	0.730(+/- 0.093)	0.638(+/- 0.095)	0.576(+/- 0.084)	0.580(+/- 0.084)
MP BOSSVS	0.721(+/- 0.095)	0.644(+/- 0.107)	0.641(+/- 0.107)	0.551(+/- 0.049)
SAX RISE	0.718(+/- 0.057)	0.630(+/- 0.083)	0.537(+/- 0.056)	0.526(+/- 0.029)
MP Gramian + Recurrence RF	0.707(+/- 0.093)	0.621(+/- 0.091)	0.628(+/- 0.099)	0.641(+/- 0.126)
Gramian ResNetV2	0.703(+/- 0.090)	0.663(+/- 0.154)	0.676(+/- 0.159)	0.506(+/- 0.029)
MP Gramian + Recurrence SVM	0.701(+/- 0.072)	0.661(+/- 0.108)	0.614(+/- 0.103)	0.569(+/- 0.048)
RISE	0.701(+/- 0.048)	0.596(+/- 0.057)	0.548(+/- 0.059)	0.545(+/- 0.047)
MP TSF	0.678(+/- 0.060)	0.576(+/- 0.046)	0.618(+/- 0.094)	0.533(+/- 0.038)
MP KNN	0.645(+/- 0.038)	0.569(+/- 0.072)	0.605(+/- 0.074)	0.524(+/- 0.044)
MP RISE	0.610(+/- 0.043)	0.504(+/- 0.017)	0.502(+/- 0.018)	0.503(+/- 0.017)
MP Gramian + Recurrence KNN	0.602(+/- 0.070)	0.548(+/- 0.049)	0.577(+/- 0.059)	0.501(+/- 0.030)
Recurrence ResNetV2	0.601(+/- 0.119)	0.622(+/- 0.142)	0.565(+/- 0.110)	0.532(+/- 0.039)

Table 8 Balanced Accuracy for all methods sorted by R3 score

name	CFI R1	CFI R2	CFI R3	CFI R4
ROCKET SVM	0.268(+/- 0.124)	0.327(+/- 0.093)	0.458(+/- 0.180)	0.543(+/- 0.142)
ROCKET RF	0.332(+/- 0.123)	0.318(+/- 0.072)	0.385(+/- 0.117)	0.543(+/- 0.106)
TS-CHIEF	0.375(+/- 0.146)	0.483(+/- 0.105)	0.701(+/- 0.180)	0.861(+/- 0.092)
KNN	0.381(+/- 0.124)	0.558(+/- 0.161)	0.550(+/- 0.083)	0.794(+/- 0.113)
SAX ROCKET RF	0.384(+/- 0.086)	0.439(+/- 0.130)	0.593(+/- 0.140)	0.576(+/- 0.123)
ROCKET KNN	0.392(+/- 0.110)	0.334(+/- 0.106)	0.435(+/- 0.181)	0.652(+/- 0.124)
ROCKET Ridge	0.401(+/- 0.080)	0.347(+/- 0.096)	0.521(+/- 0.090)	0.541(+/- 0.138)
Recurrence Flat RF	0.409(+/- 0.130)	0.412(+/- 0.104)	0.490(+/- 0.071)	0.464(+/- 0.133)
Gramian + Recurrence SVM	0.418(+/- 0.110)	0.389(+/- 0.122)	0.490(+/- 0.064)	0.526(+/- 0.128)
SAX ROCKET SVM	0.420(+/- 0.103)	0.353(+/- 0.143)	0.559(+/- 0.094)	0.579(+/- 0.134)
Gramian + Recurrence RF	0.437(+/- 0.072)	0.442(+/- 0.060)	0.459(+/- 0.093)	0.518(+/- 0.097)
TSF	0.438(+/- 0.189)	0.549(+/- 0.179)	0.646(+/- 0.159)	0.742(+/- 0.143)
Recurrence Flat SVM	0.446(+/- 0.081)	0.408(+/- 0.130)	0.508(+/- 0.097)	0.567(+/- 0.129)
Recurrence Flat Ridge	0.449(+/- 0.061)	0.479(+/- 0.059)	0.523(+/- 0.077)	0.535(+/- 0.045)
Recurrence Flat KNN	0.456(+/- 0.127)	0.471(+/- 0.118)	0.662(+/- 0.118)	0.719(+/- 0.100)
Gramian Flat KNN	0.462(+/- 0.117)	0.471(+/- 0.112)	0.657(+/- 0.128)	0.520(+/- 0.115)
SAX ROCKET Ridge	0.464(+/- 0.076)	0.365(+/- 0.110)	0.547(+/- 0.076)	0.553(+/- 0.135)
Gramian Flat RF	0.465(+/- 0.107)	0.494(+/- 0.106)	0.567(+/- 0.073)	0.521(+/- 0.110)
Gramian Flat SVM	0.466(+/- 0.088)	0.429(+/- 0.103)	0.473(+/- 0.071)	0.519(+/- 0.111)
SFA TSF	0.467(+/- 0.125)	0.612(+/- 0.149)	0.786(+/- 0.111)	0.733(+/- 0.166)
InceptionTime	0.470(+/- 0.134)	0.406(+/- 0.175)	0.636(+/- 0.232)	0.859(+/- 0.141)
SAX ROCKET KNN	0.471(+/- 0.131)	0.435(+/- 0.099)	0.672(+/- 0.077)	0.595(+/- 0.103)
Gramian + Recurrence KNN	0.472(+/- 0.135)	0.511(+/- 0.125)	0.665(+/- 0.102)	0.569(+/- 0.140)
Gramian Flat Ridge	0.479(+/- 0.064)	0.469(+/- 0.067)	0.557(+/- 0.086)	0.568(+/- 0.098)
Gramian + Recurrence Ridge	0.482(+/- 0.050)	0.470(+/- 0.074)	0.508(+/- 0.087)	0.528(+/- 0.042)
SAX TSF	0.482(+/- 0.105)	0.514(+/- 0.069)	0.745(+/- 0.120)	0.768(+/- 0.128)
SFA KNN	0.496(+/- 0.134)	0.477(+/- 0.084)	0.782(+/- 0.109)	0.702(+/- 0.116)
BOSSVS	0.504(+/- 0.058)	0.513(+/- 0.080)	0.685(+/- 0.120)	0.698(+/- 0.088)
MP ROCKET SVM	0.522(+/- 0.145)	0.601(+/- 0.200)	0.651(+/- 0.108)	0.766(+/- 0.147)
SAX KNN	0.545(+/- 0.142)	0.736(+/- 0.122)	0.648(+/- 0.137)	0.800(+/- 0.096)
MP ROCKET Ridge	0.549(+/- 0.124)	0.660(+/- 0.156)	0.673(+/- 0.131)	0.782(+/- 0.078)
MP ROCKET RF	0.559(+/- 0.156)	0.594(+/- 0.168)	0.669(+/- 0.145)	0.782(+/- 0.126)
SAX RISE	0.575(+/- 0.102)	0.744(+/- 0.153)	0.922(+/- 0.111)	0.944(+/- 0.055)
MP ROCKET KNN	0.582(+/- 0.161)	0.746(+/- 0.142)	0.838(+/- 0.144)	0.836(+/- 0.153)
SAX BOSSVS	0.583(+/- 0.078)	0.641(+/- 0.111)	0.804(+/- 0.078)	0.691(+/- 0.096)
RISE	0.610(+/- 0.088)	0.808(+/- 0.112)	0.900(+/- 0.116)	0.903(+/- 0.089)
MP Gramian + Recurrence Ridge	0.633(+/- 0.119)	0.683(+/- 0.062)	0.705(+/- 0.071)	0.766(+/- 0.070)
MP Gramian + Recurrence SVM	0.639(+/- 0.135)	0.703(+/- 0.144)	0.767(+/- 0.165)	0.836(+/- 0.072)
Gramian ResNetV2	0.640(+/- 0.144)	0.691(+/- 0.293)	0.646(+/- 0.283)	0.981(+/- 0.056)
MP Gramian + Recurrence RF	0.645(+/- 0.133)	0.768(+/- 0.123)	0.760(+/- 0.127)	0.744(+/- 0.157)
MP TSF	0.666(+/- 0.101)	0.842(+/- 0.084)	0.764(+/- 0.178)	0.924(+/- 0.070)
MP BOSSVS	0.689(+/- 0.093)	0.764(+/- 0.085)	0.769(+/- 0.080)	0.830(+/- 0.025)
MP KNN	0.720(+/- 0.074)	0.85(+/- 0.131)	0.791(+/- 0.135)	0.946(+/- 0.085)
MP RISE	0.779(+/- 0.084)	0.988(+/- 0.033)	0.988(+/- 0.033)	0.988(+/- 0.033)
MP Gramian + Recurrence KNN	0.789(+/- 0.130)	0.889(+/- 0.087)	0.838(+/- 0.095)	0.969(+/- 0.046)
Recurrence ResNetV2	0.836(+/- 0.189)	0.772(+/- 0.229)	0.858(+/- 0.163)	0.919(+/- 0.075)

Table 9 CFI for all methods sorted by R3 score

name	F1 score R1	F1 score R2	F1 score R3	F1 score R4
ROCKET SVM	0.838(+/- 0.085)	0.800(+/- 0.068)	0.683(+/- 0.164)	0.613(+/- 0.132)
ROCKET RF	0.794(+/- 0.087)	0.808(+/- 0.051)	0.754(+/- 0.086)	0.619(+/- 0.103)
SAX ROCKET RF	0.758(+/- 0.065)	0.709(+/- 0.101)	0.564(+/- 0.144)	0.584(+/- 0.121)
KNN	0.757(+/- 0.095)	0.594(+/- 0.158)	0.615(+/- 0.075)	0.325(+/- 0.165)
TS-CHIEF	0.757(+/- 0.118)	0.674(+/- 0.091)	0.430(+/- 0.218)	0.231(+/- 0.149)
ROCKET KNN	0.750(+/- 0.081)	0.794(+/- 0.072)	0.704(+/- 0.144)	0.502(+/- 0.136)
ROCKET Ridge	0.745(+/- 0.063)	0.785(+/- 0.072)	0.642(+/- 0.078)	0.615(+/- 0.141)
Recurrence Flat RF	0.733(+/- 0.107)	0.734(+/- 0.085)	0.671(+/- 0.061)	0.686(+/- 0.128)
Gramian + Recurrence SVM	0.729(+/- 0.090)	0.750(+/- 0.099)	0.672(+/- 0.057)	0.632(+/- 0.116)
SAX ROCKET SVM	0.728(+/- 0.079)	0.774(+/- 0.120)	0.605(+/- 0.090)	0.579(+/- 0.137)
Gramian + Recurrence RF	0.716(+/- 0.063)	0.713(+/- 0.050)	0.697(+/- 0.078)	0.644(+/- 0.089)
Recurrence Flat SVM	0.709(+/- 0.068)	0.734(+/- 0.103)	0.653(+/- 0.089)	0.591(+/- 0.130)
Recurrence Flat Ridge	0.707(+/- 0.049)	0.682(+/- 0.052)	0.641(+/- 0.075)	0.632(+/- 0.042)
TSF	0.701(+/- 0.145)	0.599(+/- 0.172)	0.503(+/- 0.170)	0.388(+/- 0.189)
Recurrence Flat KNN	0.695(+/- 0.104)	0.683(+/- 0.105)	0.493(+/- 0.125)	0.428(+/- 0.128)
SAX ROCKET Ridge	0.694(+/- 0.066)	0.770(+/- 0.080)	0.618(+/- 0.074)	0.604(+/- 0.133)
Gramian Flat SVM	0.691(+/- 0.075)	0.720(+/- 0.089)	0.687(+/- 0.062)	0.641(+/- 0.102)
Gramian Flat KNN	0.690(+/- 0.102)	0.684(+/- 0.094)	0.495(+/- 0.151)	0.639(+/- 0.117)
Gramian Flat RF	0.689(+/- 0.097)	0.664(+/- 0.098)	0.600(+/- 0.070)	0.639(+/- 0.101)
SFA TSF	0.686(+/- 0.106)	0.540(+/- 0.168)	0.337(+/- 0.157)	0.393(+/- 0.212)
InceptionTime	0.682(+/- 0.124)	0.729(+/- 0.145)	0.495(+/- 0.233)	0.222(+/- 0.204)
Gramian Flat Ridge	0.682(+/- 0.054)	0.690(+/- 0.057)	0.608(+/- 0.087)	0.596(+/- 0.101)
Gramian + Recurrence KNN	0.681(+/- 0.111)	0.645(+/- 0.125)	0.492(+/- 0.120)	0.588(+/- 0.141)
SAX ROCKET KNN	0.681(+/- 0.108)	0.716(+/- 0.087)	0.488(+/- 0.086)	0.568(+/- 0.103)
Gramian + Recurrence Ridge	0.680(+/- 0.042)	0.689(+/- 0.062)	0.653(+/- 0.078)	0.639(+/- 0.037)
SAX TSF	0.675(+/- 0.096)	0.650(+/- 0.062)	0.389(+/- 0.167)	0.358(+/- 0.172)
BOSSVS	0.660(+/- 0.050)	0.650(+/- 0.074)	0.465(+/- 0.138)	0.456(+/- 0.101)
SFA KNN	0.658(+/- 0.126)	0.682(+/- 0.074)	0.344(+/- 0.148)	0.446(+/- 0.142)
MP ROCKET SVM	0.633(+/- 0.127)	0.540(+/- 0.205)	0.507(+/- 0.123)	0.353(+/- 0.204)
MP ROCKET Ridge	0.611(+/- 0.117)	0.485(+/- 0.182)	0.475(+/- 0.171)	0.350(+/- 0.108)
SAX KNN	0.609(+/- 0.156)	0.402(+/- 0.154)	0.504(+/- 0.147)	0.322(+/- 0.131)
MP ROCKET RF	0.595(+/- 0.149)	0.554(+/- 0.188)	0.475(+/- 0.189)	0.338(+/- 0.173)
SAX RISE	0.587(+/- 0.107)	0.385(+/- 0.182)	0.126(+/- 0.173)	0.099(+/- 0.099)
SAX BOSSVS	0.583(+/- 0.076)	0.518(+/- 0.117)	0.320(+/- 0.110)	0.463(+/- 0.119)
MP ROCKET KNN	0.569(+/- 0.175)	0.383(+/- 0.189)	0.253(+/- 0.197)	0.251(+/- 0.228)
RISE	0.554(+/- 0.096)	0.304(+/- 0.171)	0.162(+/- 0.181)	0.164(+/- 0.147)
MP Gramian + Recurrence Ridge	0.522(+/- 0.151)	0.477(+/- 0.076)	0.450(+/- 0.085)	0.372(+/- 0.095)
MP Gramian + Recurrence SVM	0.516(+/- 0.140)	0.436(+/- 0.189)	0.350(+/- 0.204)	0.275(+/- 0.101)
Gramian ResNetV2	0.513(+/- 0.158)	0.404(+/- 0.308)	0.452(+/- 0.341)	0.032(+/- 0.095)
MP Gramian + Recurrence RF	0.507(+/- 0.160)	0.358(+/- 0.168)	0.368(+/- 0.175)	0.384(+/- 0.186)
MP TSF	0.491(+/- 0.120)	0.263(+/- 0.129)	0.347(+/- 0.236)	0.132(+/- 0.119)
MP BOSSVS	0.466(+/- 0.114)	0.373(+/- 0.111)	0.367(+/- 0.105)	0.289(+/- 0.038)
MP KNN	0.432(+/- 0.087)	0.239(+/- 0.191)	0.325(+/- 0.180)	0.089(+/- 0.142)
MP RISE	0.353(+/- 0.115)	0.019(+/- 0.059)	0.019(+/- 0.059)	0.019(+/- 0.059)
MP Gramian + Recurrence KNN	0.327(+/- 0.181)	0.187(+/- 0.143)	0.265(+/- 0.143)	0.054(+/- 0.084)
Recurrence ResNetV2	0.239(+/- 0.265)	0.317(+/- 0.293)	0.216(+/- 0.229)	0.141(+/- 0.128)

Table 10 F1 Score for all methods sorted by R3 score

name	Min-Max Normalization	Feature Selection (Top 100)	Model Parameters
KNN	0	0	$k = 7$, $weight = 1/d$
SAX KNN	0	0	$k = 7$, $weight = 1/d$
SFA KNN	0	0	$k = 7$, $weight = 1/d$
MP KNN	0	0	$k = 7$, $weight = 1/d$
Recurrence Flat KNN	1	1	$k = 7$, $weight = 1/d$
Gramian Flat KNN	1	1	$k = 7$, $weight = 1/d$
Gramian + Recurrence KNN	1	1	$k = 7$, $weight = 1/d$
MP Gramian + Recurrence KNN	1	1	$k = 7$, $weight = 1/d$
ROCKET KNN	1	1	$k = 7$, $weight = 1/d$
MP ROCKET KNN	1	1	$k = 7$, $weight = 1/d$
SAX ROCKET KNN	1	1	$k = 7$, $weight = 1/d$
Recurrence Flat Ridge	1	1	$\alpha = 10$, $\tau = 0.001$
Gramian Flat Ridge	1	1	$\alpha = 10$, $\tau = 0.001$
Gramian + Recurrence Ridge	1	1	$\alpha = 10$, $\tau = 0.001$
MP Gramian + Recurrence Ridge	1	1	$\alpha = 10$, $\tau = 0.001$
ROCKET Ridge	1	1	$\alpha = 10$, $\tau = 0.001$
MP ROCKET Ridge	1	1	$\alpha = 10$, $\tau = 0.001$
SAX ROCKET Ridge	1	1	$\alpha = 10$, $\tau = 0.001$
TSF	0	0	$n_trees = 300$
SFA TSF	0	0	$n_trees = 300$
MP TSF	0	0	$n_trees = 300$
SAX TSF	0	0	$n_trees = 300$
BOSSVS	0	0	$n_trees = 300$
SAX BOSSVS	0	0	$n_trees = 300$
MP BOSSVS	0	0	$n_trees = 300$
Recurrence Flat SVM	1	1	$word_size = 5$, $n_bins = 5$, $window_size = 0.15$
Gramian Flat SVM	1	1	$word_size = 5$, $n_bins = 5$, $window_size = 0.15$
MP Gramian + Recurrence SVM	1	1	$word_size = 5$, $n_bins = 5$, $window_size = 0.15$
ROCKET SVM	1	1	$C = 10$, $kernel = rbf$
SAX ROCKET SVM	1	1	$C = 10$, $kernel = rbf$
MP ROCKET SVM	1	1	$C = 10$, $kernel = rbf$
Recurrence Flat RF	0	0	$C = 10$, $kernel = rbf$
Gramian Flat RF	0	0	$C = 10$, $kernel = rbf$
Gramian + Recurrence RF	0	0	$C = 10$, $kernel = rbf$
MP Gramian + Recurrence RF	0	0	$C = 10$, $kernel = rbf$
ROCKET RF	1	1	$C = 10$, $kernel = rbf$
SAX ROCKET RF	1	1	$C = 10$, $kernel = rbf$
MP ROCKET RF	1	1	$C = 10$, $kernel = rbf$
RISE	0	0	$n_trees = 300$, $max_depth = None$, $max_samples = 0.75$, $ccp_alpha = 0.022$
SAX RISE	0	0	$n_trees = 300$, $max_depth = None$, $max_samples = 0.75$, $ccp_alpha = 0.022$
MP RISE	0	0	$n_trees = 300$, $max_depth = None$, $max_samples = 0.75$, $ccp_alpha = 0.022$
InceptionTime	0	0	$n_trees = 300$, $max_depth = None$, $max_samples = 0.75$, $ccp_alpha = 0.022$
TS CHIEF	0	0	$n_trees = 300$, $max_depth = None$, $max_samples = 0.75$, $ccp_alpha = 0.022$
Recurrence ResNetV2	0	0	$n_trees = 300$, $max_depth = None$, $max_samples = 0.75$, $ccp_alpha = 0.022$
Gramian ResNetV2	0	0	$n_trees = 300$, $max_depth = None$, $max_samples = 0.75$, $ccp_alpha = 0.022$

Table 11 Parameters of each classifier, and if they use Min-Max normalization and/or feature selection (with Extra Trees)

name	Parameters
SAX	$n_bins = 5$, $strategy = uniform$
SFA	$n_coefs = 10$, $n_bins = 5$, $strategy = uniform$, $drop_sum = True$, $anova = True$
Recurrence	$img_size = 128 * 128$, $dimension = 1$, $time_delay = 6$
Gramian	$img_size = 128 * 128$
MP	$window_size = 0.15$
ROCKET	$n_kernels = 20000$, $kernel_sizes = (5, 7, 9, 11)$

Table 12 Parameters of the representations methods